UNCERTAINTY MODELS FOR PHYSICALLY REALIZABLE INERTIA DYADICS

Mason A. Peck[*]

ABSTRACT

This paper proposes new probability-distribution functions (PDFs) for the inertia dyadic. Representing uncertainty in rigid-body rotational dynamics with these PDFs preserves constraints on the moments and products of inertia that arise from the underlying physics but which conventional approaches violate. Specifically, we propose representing uncertainty in terms of parameters closely related to the radii of gyration and in terms of Euler parameters (for the orientation of the principal axes with respect to a set of body-fixed reference coordinates). The physical constraints on the moments and products of inertia are shown to be satisfied for any distribution of the radii of gyration and if the Euler parameters are given a radially constrained Gaussian distribution. Although unconventional, this uncertainty structure is shown to be broadly applicable. We consider the example of spacecraft/launch-vehicle separation analysis for an early-stage spacecraft program, when mass properties are ill defined. Here, misplaced conservatism in requirements can be costly. The proposed PDFs are shown to guarantee physically realizable results, while more naïve approaches yield nonphysical behaviors.

INTRODUCTION

Successful spacecraft designs accommodate uncertainty in the inertia properties of the system and its components. These parameters are difficult to measure precisely even when the components of the spacecraft have been fully integrated, let alone to predict with much confidence in the early stages of the design when, inconveniently, much of the engineering analysis that requires inertia estimates occurs. An obvious example of the use of statistical inertia models is attitude-control performance in the presence of plant uncertainty. However, no less important are other uses of these models, including nonlinear Monte Carlo simulations, mass-properties bounds used early in the product design cycle, and generic representations of a satellite product line as part of specifying interfaces with subcontractors, such as launch-vehicle providers. These applications often attempt to accommodate

---

large uncertainties in mass properties, so large that (we argue) the way they are specified risks introducing artificial and costly conservatism.

A standard approach to the problem of representing inertia uncertainty is to treat each of the six unique entries in an inertia matrix as independent random variates, each of which exhibits some completely uncorrelated uncertainty. This approach has the virtue of simplicity, and for small uncertainties it is—if not correct—at least difficult to distinguish from the truth. Instead, we propose a rigorous approach to uncertainty modeling in rigid-body rotational dynamics that not only recognizes the interdependency of the inertia parameters but also allows arbitrarily large uncertainties that do not violate the physical principles from which the inertia matrix is derived.

INERTIA DYADICS

We consider an inertia dyadic $\boldsymbol{I}$

$$\boldsymbol{I} = I_{11}\boldsymbol{b}_1\boldsymbol{b}_1 + I_{22}\boldsymbol{b}_1\boldsymbol{b}_1 + I_{33}\boldsymbol{b}_1\boldsymbol{b}_1 + I_{12}\left(\boldsymbol{b}_1\boldsymbol{b}_2 + \boldsymbol{b}_2\boldsymbol{b}_1\right) + I_{13}\left(\boldsymbol{b}_1\boldsymbol{b}_3 + \boldsymbol{b}_3\boldsymbol{b}_1\right) + I_{23}\left(\boldsymbol{b}_2\boldsymbol{b}_3 + \boldsymbol{b}_3\boldsymbol{b}_2\right) = \begin{bmatrix}\boldsymbol{b}_1 & \boldsymbol{b}_2 & \boldsymbol{b}_3\end{bmatrix}I\begin{bmatrix}\boldsymbol{b}_1 \\ \boldsymbol{b}_2 \\ \boldsymbol{b}_3\end{bmatrix}, \tag{1}$$

in terms of some orthogonal basis vectors $\boldsymbol{b}_i$ in a body-fixed frame B. The inertia matrix I contains the scalars in this vector expression, for some choice of $\boldsymbol{b}_i$:

$$I = \begin{bmatrix} I_{11} & I_{12} & I_{13} \\ I_{12} & I_{22} & I_{23} \\ I_{13} & I_{23} & I_{33} \end{bmatrix}, \tag{2}$$

in which the I_{ii} are known as the moments of inertia and are given by a Riemann integral over M, in terms of a differential mass element dm and that element's location (x_1, x_2, x_3) in a reference coordinate system determined by the $\boldsymbol{b}_i$ [1]:

$$\begin{aligned} I_{11} &\equiv \int_M \left(x_2^2 + x_3^2\right)dm \\ I_{22} &\equiv \int_M \left(x_1^2 + x_3^2\right)dm \,. \\ I_{33} &\equiv \int_M \left(x_1^2 + x_2^2\right)dm \end{aligned} \tag{3}$$

The I_{ij} are known as the products of inertia and are given by

$$I_{12} \equiv -\int_M x_1 x_2 \, dm$$

$$I_{13} \equiv -\int_M x_1 x_3 \, dm \ . \tag{4}$$

$$I_{23} \equiv -\int_M x_2 x_3 \, dm$$

Since I is positive definite in practice, it can always be diagonalized. The similarity transform A, nothing more than a collection of the eigenvectors of I, is a proper-orthogonal matrix that describes the orientation of the principal coordinates P with respect to B such that the principal (or diagonal) inertia matrix is

$$I_p \equiv \begin{bmatrix} I_1 & 0 & 0 \\ 0 & I_2 & 0 \\ 0 & 0 & I_3 \end{bmatrix} = A^{\mathrm{T}} I A \, , \tag{5}$$

i.e.,

$$\boldsymbol{I} = I_1 \boldsymbol{p}_1 \boldsymbol{p}_1 + I_2 \boldsymbol{p}_2 \boldsymbol{p}_2 + I_3 \boldsymbol{p}_3 \boldsymbol{p}_3 \tag{6}$$

Criteria for Physical Realizability

Because I is real and symmetric, it contains no more than 6 unique parameters. These parameters can be taken to consist of the I_{ii} and the I_{ij} or, equivalently the three principal moments of inertia I_i and the attitude representation A. A proper-orthogonal matrix is a member of the $SO(3)$ rotation group and can be represented with three parameters [2]. Thus, the I_i taken together with three attitude parameters comprise a different, although equally complete, set of 6 parameters. The parameters in the inertia matrix obey certain constraints, all of which are evident from the above definitions:

- The moments of inertia of $A^{\mathrm{T}} I A$ must be positive, regardless of the matrix A that rotates the inertia matrix (whether A contains the eigenvectors of I or represents some other proper-orthogonal matrix).

- The sum of any two moments must be less than or equal to the third. This principle is known as the *triangle inequality* for inertia matrices, because the sides of a triangle also obey this rule.

- The products of inertia are limited by the simultaneous application of both of the above constraints.

We now derive a simple test for these conditions. We rewrite the I_i in terms of three independent scalars, K_k, such that

$$I_1 = K_2 + K_3$$
$$I_2 = K_1 + K_3 \tag{7}$$
$$I_3 = K_1 + K_2$$

or

$$\begin{bmatrix} K_1 \\ K_2 \\ K_3 \end{bmatrix} = \frac{1}{2} \begin{bmatrix} -1 & 1 & 1 \\ 1 & -1 & 1 \\ 1 & 1 & -1 \end{bmatrix} \begin{bmatrix} I_1 \\ I_2 \\ I_3 \end{bmatrix}. \tag{8}$$

We conclude from equation (7) that the principal inertia matrix will obey the triangle inequality if all of the K_k take on positive values. From equation (3)

$$K_k \equiv \int_M x_k^2 \, dm \, . \tag{9}$$

Therefore, they are related in a simple way to the radii of gyration. Furthermore, we now have a simple way to assess the physical realizability of a given matrix. Because the physics are independent of the choice of coordinates, any matrix with negative K_k includes physically unrealizable moments of inertia, products of inertia, or both, in every possible coordinate system.

UNCERTAINTY

The inertia dyadic is independent of the choice of the b_i. The components I_{ii} and I_{ij} may change, but not $\textbf{\textit{I}}$. Therefore, uncertainty in the inertia dyadic must be independent of the inertia matrix, which is merely a realization of the dyadic in some reference coordinates. Having recognized this fundamental principle, we can separate uncertainty into two decoupled problems: the uncertainty in the principal moments of inertia and uncertainty in A.

Picking Principal Inertias from a Distribution

We require a method for choosing a random inertia-matrix variate whose components conform to the limits of physical realizability. Simply picking three numbers from an arbitrary probability distribution does not guarantee that the resulting values are legitimate principal moments of inertia. To this end, we assign uncorrelated zero-mean stochastic processes w_k to the square root k_k of each K_k:

$$\begin{bmatrix} \hat{k}_1 \\ \hat{k}_2 \\ \hat{k}_3 \end{bmatrix} = \begin{bmatrix} \sqrt{\hat{K}_1} \\ \sqrt{\hat{K}_2} \\ \sqrt{\hat{K}_3} \end{bmatrix} = \begin{bmatrix} \bar{k}_1 + w_1 \\ \bar{k}_2 + w_2 \\ \bar{k}_3 + w_3 \end{bmatrix}. \tag{10}$$

Squaring each value then results in a positive number, regardless of the variance. If the distribution in k_k is Gaussian, for example, the resulting K_k can be described with a Chi-squared distribution [3]. We have already demonstrated that any inertia matrix derived from these parameters is positive definite. Transforming into the random principal moments of inertia $\hat{I}_i$ involves only

$$\begin{bmatrix} \hat{I}_1 \\ \hat{I}_2 \\ \hat{I}_3 \end{bmatrix} = \begin{bmatrix} 0 & 1 & 1 \\ 1 & 0 & 1 \\ 1 & 1 & 0 \end{bmatrix} \begin{bmatrix} \hat{K}_1 \\ \hat{K}_2 \\ \hat{K}_3 \end{bmatrix}. \tag{11}$$

Extracting the statistics of some sampled inertia matrices for use in this model requires only fitting a Chi-squared distribution to the three k_k that characterize each sample.

Uncertainty in Principal Coordinates

Devising a successful algorithm for picking uniformly random attitudes is not a trivial matter. One reason is that applying a uniform distribution to each of the attitude parameters in a given parameterization (such as Euler angles, Rodrigues parameters, and direction-cosine matrix components) is generally inappropriate: doing so introduces biases that are evident when one transforms from one parameterization to another [4]. Several recent studies address the issue of picking random attitudes. Shuster points out that the distribution of attitude should be independent of the attitude representation [5]. He derives probability density functions for several attitude parameterizations and shows that they comply with this axiom. Like Shuster, most authors consider the problem of uniform attitude distributions, often with an eye toward Bayesian attitude estimation. In addition to Shuster's, other successful algorithms for picking uniformly distributed attitudes include the igloo and masonry maps [6], iterative selection of quaternions based on a box criterion [4], and picking points on a unit four sphere [4,7]. The latter technique provides uniformly distributed unit quaternions. It consists of selecting normally distributed vectors in R^4 (i.e. selecting four uncorrelated, normally distributed real numbers) and enforcing the unity-magnitude constraint. This simple algorithm may be the most convenient one for numerical simulation because the coding is minimal and requires neither trigonometric computations nor conditional statements.

Representing a uniformly distributed inertia matrix may be of interest in some applications. For example, statistically demonstrating an adaptive attitude-tracking algorithm that purports to require no knowledge of the inertia matrix might require arbitrary plant models [8]. However, other distributions are required if one wishes to represent the statistics of rigid-body mass properties that exhibit central tendencies. For this situation, we turn to the concept of a radially constrained Gaussian (RCG), first proposed by Nicewarner and Sanderson [9]. Their approach provides a way to represent general orientational uncertainty for both two- and three-dimensional problems. They also incorporate positional uncertainty via the homogeneous transform [10]. The general technique begins with an n dimensional vector x with a probability density function

$$f_x(x) = \frac{1}{(2\pi)^{\frac{n}{2}} |\Sigma|^{\frac{1}{2}}} \exp\left\{-\frac{1}{2}(x-\hat{x})^T \Sigma^{-1}(x-\hat{x})\right\} \tag{12}$$

where n is the dimension of the random vector, Σ is the covariance matrix, and $\hat{x}$ is the mean. One can enforce the constraint of unit length by decomposing k components of x into hyperspectral coordinates

$$
\begin{aligned}
x_1 &= r\sin\theta_1 \sin\theta_2 \cdots \sin\theta_{k-2} \cos\theta_{k-1} \\
x_2 &= r\sin\theta_1 \sin\theta_2 \cdots \sin\theta_{k-2} \sin\theta_{k-1} \\
x_3 &= r\sin\theta_1 \sin\theta_2 \cdots \sin\theta_{k-3} \cos\theta_{k-2} \\
&\vdots \\
x_{k-2} &= r\sin\theta_1 \sin\theta_2 \cos\theta_3 \\
x_{k-1} &= r\sin\theta_1 \cos\theta_2 \\
x_k &= r\cos\theta_1 \\
x_{k+1} &= s_1 \\
x_{k+2} &= s_2 \\
&\vdots \\
x_n &= s_{n-k}
\end{aligned}
\tag{13}
$$

and normalizing by dividing by r. Here,

$$
\begin{aligned}
0 &< \theta_i < \pi, \qquad i = 1...k\text{-}2 \\
0 &< \theta_{k-1} < 2\pi.
\end{aligned}
\tag{14}
$$

This transformation $x = g(\Phi, r)$ from a vector Φ (comprising the k-1 angles θ and the n-k spatial components s) has as its Jacobian

$$J(\Phi,r) = \begin{bmatrix} \dfrac{\partial g_1}{\partial \phi_1} & \cdots & \dfrac{\partial g_1}{\partial \phi_{n-1}} & \dfrac{\partial g_1}{\partial r} \\ \vdots & \ddots & \vdots & \vdots \\ \dfrac{\partial g_n}{\partial \phi_1} & \cdots & \dfrac{\partial g_n}{\partial \phi_{n-1}} & \dfrac{\partial g_n}{\partial r} \end{bmatrix}, \tag{15}$$

the determinant of which can be shown to be

$$\Delta(\Phi,r) = r^{k-1} \sin^{k-2}\theta_1 \sin^{k-3}\theta_2 \cdots \sin^2\theta_{k-3} \sin\theta_{k-2}, \tag{16}$$

positive for all values of r and θ_{k-1} over the manifold described by equation (14).

The transformed probability distribution of the Euclidean Gaussian becomes

$$f_{\Phi,r}(\Phi,r) = \Delta(\Phi,r) f_x\big(g(\Phi,r)\big), \tag{17}$$

and the conditional probability distribution, given that $r=1$, is

$$f_\Phi\big(\Phi|\{r=1\}\big) = \frac{f_{\Phi,r}(\Phi,1)}{f_r(1)}, \tag{18}$$

Here, $f_r(r)$ is the marginal PDF

$$f_r(r) = \int_\Phi f_{\Phi,r}(\Phi,r)d\Phi. \tag{19}$$

Letting $e(\Phi) = g(\Phi) - \overline{x}$, where the mean $\overline{x}$ is assumed always to lie on the constraint manifold, leads to the PDF

$$f_\Phi(\Phi) = c\Delta(\Phi)\exp\left[-\frac{1}{2}e(\Phi)^T \Sigma^{-1} e(\Phi)\right], \tag{20}$$

where the normalization constant c is given by

$$c = \frac{1}{\displaystyle\int_\Phi \Delta(\Phi)\exp\left[-\frac{1}{2}e(\Phi)^T \Sigma^{-1} e(\Phi)\right]d\Phi}. \tag{21}$$

This distribution is that of the probability of a measurement of the hyperspectral parameters Φ. However, it is Gaussian on the vector x transformed from these parameters when the trigonometric terms from the Jacobian determinant are incorporated. Nicewarner and Sanderson also point out that the mean and covariance are coupled because the covariance matrix is applied to the transformed vector in Euclidean space, not to the radially constrained manifold. They propose eliminating this effect, if necessary, by rotating the covariance matrix via

$$R_J(\Phi) = \begin{bmatrix} n_{\Phi_1} & n_{\Phi_2} & \cdots & n_{\Phi_{n-1}} & n_r \end{bmatrix}$$
$$n_u = \frac{g_u}{|g_u|}, \quad \text{and} \quad g_u = \left.\frac{\partial g}{\partial u}\right|_{r=1} \tag{22}$$

So that

$$\Sigma = R_J(\hat{\Phi})\,\bar{\Sigma}\,R_J(\hat{\Phi})^T. \tag{23}$$

Our objectives do not extend to the case of nonzero spatial coordinates s. For random unit quaternions the transformation is

$$
\begin{aligned}
x_1 &= r\sin\theta_1 \sin\theta_2 \cos\theta_3 \\
x_2 &= r\sin\theta_1 \sin\theta_2 \sin\theta_3 \\
x_3 &= r\sin\theta_1 \cos\theta_2 \\
x_4 &= r\cos\theta_1.
\end{aligned}
\tag{24}
$$

The Jacobian determinant for $\Phi = \begin{bmatrix} \theta_1 & \theta_2 & \theta_3 \end{bmatrix}^T$ is

$$\Delta(\Phi, r) = r^3 \sin^2\theta_1 \sin\theta_2, \tag{25}$$

and the RCG PDF for a unit quaternion is therefore

$$f(\Phi) = c\sin^2\theta_1 \sin\theta_2 \exp\left[-\frac{1}{2}e(\Phi)^T \Sigma^{-1} e(\Phi)\right]. \tag{26}$$

This result provides a means of representing uncertainty in the principal coordinates of an inertia matrix when there is some central tendency. Uniformly distributed attitudes do not offer this feature.

As an example, we pick 2000 random unit quaternions and represent them graphically as variation in unit coordinate axes. Figure 1 shows the distributions for

$$\bar{e} = \begin{bmatrix} 0.0249 & 0.0005 & -0.0100 & 0.9996 \end{bmatrix}^T \text{ and } \Sigma = \begin{bmatrix} 0.00002 & 0 & 0 & 0 \\ 0 & 0.0006 & 0 & 0 \\ 0 & 0 & 0.0006 & 0 \\ 0 & 0 & 0 & 0.6 \end{bmatrix}. \tag{27}$$
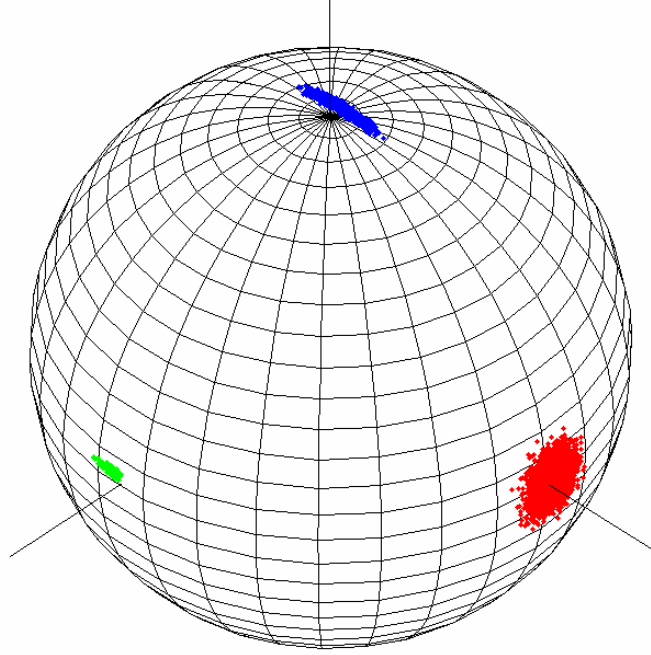
Figure 1. Random Attitudes for an Example Mean and Variance, Depicted

as Variation in Orthogonal Reference Axes

APPLICATION

This study is motivated in part by the unavailability of meaningful inertia-uncertainty models, particularly for use in the simulation of intricate dynamical processes that do not lend themselves readily to closed-form solutions. Monte Carlo simulation is often favored for analyses of this type [11]. For such problems, many statistically representative simulations are run and statistical inferences drawn from the result. Just how the statistics of the inputs are related to those of the outputs is rarely clear, although often intuitively obvious behaviors can be identified. For such an application, the complexity or inconvenience of statistical models is rarely an issue because the input parameters are picked numerically. Instead, the correctness of the statistics is paramount. Furthermore, for systems whose complexity merits statistical simulation, the computational effort involved in picking inputs from distributions is likely far less than that devoted to integrating the equations of motion. We argue that the statistical models proposed in this study proposes have a place in such analysis, although they are more cumbersome than the traditional application of Gaussian statistical models to each moment and product of inertia. The purpose of the following example is to show how the proposed uncertainty model can improve the output statistics of an intricate dynamic process, as suggested in Figure 1, which justifies their use.
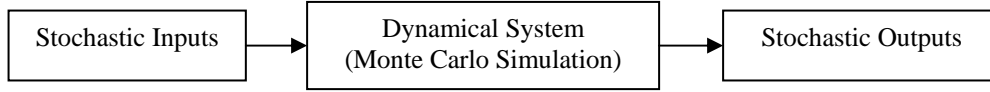
Stochastic Inputs	→	Dynamical System (Monte Carlo Simulation)	→	Stochastic Outputs

Figure 1. Arbitrary Dynamical System that Transforms Stochastic Inputs into Stochastic Outputs

Separation Analysis

Spacecraft/launch-vehicle separation is an example of a statistically intensive problem. *Separation* refers to the maneuver in which the launch vehicle's upper stage disengages from its spacecraft payload, imparting some desired dynamical condition. Commonly the maneuver is designed so that the spacecraft inherits a roll angular rate—that is, an angular velocity about the launch vehicle's longitudinal axis. In some cases, such as the Ariane 44LP / Intelsat VII separation, the upper stage separates the spacecraft with virtually no roll rate but, with the help of unbalanced springs, imparts a transverse spin instead [12]. The ensuing dynamics must typically meet requirements related to mechanical clearance (no recontact of the spacecraft and the upper stage), spin speed, nutation, and sun- or earth-relative attitude. For example, too large a nutation angle can tilt the solar panels away from the sun, affecting power safety; also, large-angle attitude motions can interrupt communications with the ground, leading to difficult and unsafe operations. Although the rigid-body equations of motion are simple enough, subtleties in the design of separation springs and clamps, umbilical connectors, and variation in the separation-system performance generally demand statistical simulation.

The example we consider here includes an oblate upper stage and a spacecraft (its payload) to be given a spin rate about a transverse axis, as was the case for Intelsat VII. Figure 3 is a schematic of such a system.
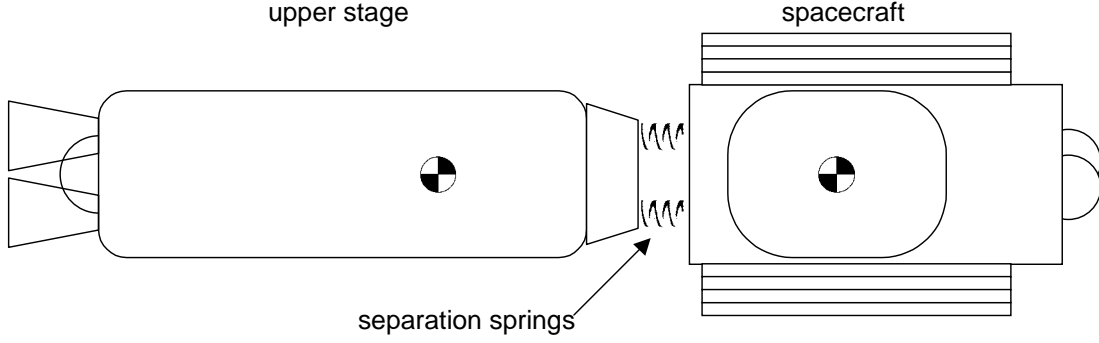
Figure 3. Upper Stage and Spacecraft

We assume four massless separation springs. Each imparts a force between the two bodies at fixed points; i.e., as the bodies separate, these points remain fixed on their respective bodies. The springs are initially compressed, and once a spring reaches its undeflected length, contact at its endpoints is assumed to be lost permanently. Two springs on one side of the spacecraft store more energy than do the other two, resulting in a couple that imparts opposite torques to the spacecraft and the upper stage. The state derivatives integrated in the simulation are

$$\frac{{}^{P}d^2\boldsymbol{c}_P}{dt^2} = -\frac{1}{m_P}\sum_{i=1}^{4}k_i\boldsymbol{x}_i$$

$$\frac{{}^{L}d^2\boldsymbol{c}_L}{dt^2} = -\frac{1}{m_L}\sum_{i=1}^{4}k_i\boldsymbol{x}_i \tag{28}$$

$$\frac{{}^{N}d\boldsymbol{\omega}^{P/N}}{dt} = \boldsymbol{I}_P^{-1}\cdot\left(-\boldsymbol{\omega}^{P/N}\times\boldsymbol{I}_P\cdot\boldsymbol{\omega}^{P/N}-\sum_{i=1}^{4}\boldsymbol{r}_{P,i}\times k_i\boldsymbol{x}_i\right)$$

$$\frac{{}^{N}d\boldsymbol{\omega}^{L/N}}{dt} = \boldsymbol{I}_L^{-1}\cdot\left(-\boldsymbol{\omega}^{L/N}\times\boldsymbol{I}_L\cdot\boldsymbol{\omega}^{L/N}+\sum_{i=1}^{4}\boldsymbol{r}_{L,i}\times k_i\boldsymbol{x}_i\right)$$

where

$$\boldsymbol{x}_i = \frac{\delta_{i,\max}-\left\|\left(\boldsymbol{c}_P-\boldsymbol{c}_L\right)+\boldsymbol{r}_{P,i}-\boldsymbol{r}_{L,i}\right\|}{\left\|\left(\boldsymbol{c}_P-\boldsymbol{c}_L\right)+\boldsymbol{r}_{P,i}-\boldsymbol{r}_{L,i}\right\|}\left[\left(\boldsymbol{c}_P-\boldsymbol{c}_L\right)+\boldsymbol{r}_{P,i}-\boldsymbol{r}_{L,i}\right]. \tag{29}$$

The superscript N indicates a derivative taken with respect to a Newtonian, or inertial, frame. The subscripts P and L indicate parameters associated with the payload and the launch vehicle, respectively. $\boldsymbol{c}$ is the position of the body mass center relative to an origin fixed in N, and m is the body's mass. The k_i are the stiffnesses of the four separation springs. The $\boldsymbol{x}_i$ are vectors parallel to the spring lines of action. The length of each $\boldsymbol{x}_i$ is the deflected length of the spring (so that when the magnitude goes to zero, no force is applied). $\delta_{i,\max}$ is the initial deflection of each spring, which is assumed to be positive and nonzero. The $\boldsymbol{r}_i$ are vectors from a body's mass center to the fixed

points on that body at which the separation springs apply forces. $\boldsymbol{\omega}^{P/N}$ is the angular velocity of a frame P, fixed in the spacecraft, relative to N. Similarly, $\boldsymbol{\omega}^{L/N}$ is the launch-vehicle rate in N. $\boldsymbol{I}$ is the inertia dyadic of the body for its mass center.

Velocities are integrated from these accelerations, and position from these velocities. In the case of angular displacement, the angular velocity of each body is integrated via a quaternion, taken to be the identity rotation at the beginning of the simulation. The resulting body-to-inertial attitudes are used to resolve the vectors in equation (29) into components in convenient coordinate systems. Table 1 lists the mean values for these system parameters. In the simulations, only the inertia dyadics are varied. In practice, all of these parameters, and many more we have omitted from this simulation, would be subject to randomization.

Table 1. Simulation Parameters

Parameter	Units	Value		
I_P	kg·m^2	5000	20	2
		20	4000	-50
		2	-50	3000
I_L	kg·m^2	6700	0	20
		0	6700	-20
		20	-20	2000
m_P	kg·	10000		
m_L	kg·	4000		
k_1, k_2	N/m	1×10^5		
k_3, k_4	N/m	3×10^4		
$\delta_{i,max}$	m	0.1		
c_P (t=0)	m	$[\,0\ 0\ 1\,]^T$		
c_L (t=0)	m	$[\,0\ 0\ -1\,]^T$		
$\boldsymbol{\omega}^{P/N}$ (t=0)	rad/sec	$[\,0\ 0\ 0\,]^T$		
$\boldsymbol{\omega}^{L/N}$ (t=0)	rad/sec	$[\,0\ 0\ 0\,]^T$		

The covariance of the RCG quaternion for both I_P and I_L is chosen to be

$$\Sigma = \begin{bmatrix} 0.00002 & 0 & 0 & 0 \\ 0 & 0.0006 & 0 & 0 \\ 0 & 0 & 0.0006 & 0 \\ 0 & 0 & 0 & 0.6 \end{bmatrix}. \tag{30}$$

Because the first three quaternion components include so little variation (a standard deviation of about 2.8° in total angle), variation in the fourth will largely be constrained out on the spherical manifold. The covariance in the radii of gyration are chosen as

$$V_{K_L} = \begin{bmatrix} 0.0067 & 0 & 0 \\ 0 & 0.0067 & 0 \\ 0 & 0 & 0.002 \end{bmatrix} \quad V_{K_P} = \begin{bmatrix} 0.125 & 0 & 0 \\ 0 & 0.1 & 0 \\ 0 & 0 & 0.75 \end{bmatrix}, \tag{31}$$

which reflects greater certainty in the launch-vehicle inertia parameters than in the spacecraft's. The implication is that the spacecraft's design is less mature at the phase in its design at which this analysis is performed. Alternatively, this analysis might be meant to capture the general behavior of a commercial spacecraft product line for a given launch vehicle. The mean and variance of the principal-axis parameters is shown in Figure 1.

The behaviors of interest here are those associated with the payload's post-separation spinning attitude dynamics: wobble, nutation, and coning. Given an intended spin axis in reference coordinates $s=[1\ 0\ 0]^T$, we define wobble as the angle between this axis and the nearest principal axis of the inertia matrix. More precisely, for appropriately sorted eigenvectors,

$$A = \begin{bmatrix} a_1 & a_2 & a_3 \end{bmatrix}, \tag{32}$$

the wobble angle ϕ is

$$\phi = \cos^{-1}\left(\begin{bmatrix} 1 & 0 & 0 \end{bmatrix} a_1 \right). \tag{33}$$

For unforced motion, nutation refers to the behavior of the angular-momentum vector as it orbits a relative equilibrium [13] in body axes. Also called free precession, this phenomenon can occur only about an equilibrium corresponding to the axis of maximum or minimum inertia. In an inertial frame, it is the principal axis that precesses around the fixed angular momentum. In either case, the nutation angle θ for an inertia dyadic I and an angular velocity vector ω is

$$\theta = \cos^{-1}\left(\frac{a_1 \cdot I \cdot \omega}{\|I \cdot \omega\|} \right). \tag{34}$$

When the transverse principal moments of inertia (i.e. those other than spin, in this case 2 and 3) are unequal, the nutation angle varies in time and depends on the proximity of the angular-velocity vector to these transverse principal axes. It is a simple matter to show that θ is at a maximum when the angular velocity vector is closest to the intermediate axis. By manipulation of expressions for kinetic energy $2E = \omega \cdot I \cdot \omega$ and angular momentum $H = I \cdot \omega$, one can derive closed-form expressions for these extrema:

$$\theta_2 = \cos^{-1}\left(\left|\frac{\left|I_1\left(2EI_2 - \boldsymbol{H}\cdot\boldsymbol{H}\right)\right|^{\frac{1}{2}}}{\left(I_2 - I_1\right)\boldsymbol{H}\cdot\boldsymbol{H}}\right|\right), \quad \theta_3 = \cos^{-1}\left(\left|\frac{\left|I_1\left(2EI_3 - \boldsymbol{H}\cdot\boldsymbol{H}\right)\right|^{\frac{1}{2}}}{\left(I_3 - I_1\right)\boldsymbol{H}\cdot\boldsymbol{H}}\right|\right). \tag{35}$$

Again, these expressions are meaningful only when the spin moment of inertia is not the intermediate. The cone angle ψ is the combined effect of these two. It is the angle between the intended spin axis and the angular momentum vector:

$$\psi = \cos^{-1}\left(\frac{\begin{bmatrix} 1 & 0 & 0 \end{bmatrix}I\omega}{\|\boldsymbol{I}\cdot\boldsymbol{\omega}\|}\right). \tag{36}$$

The wobble angle is a measure of the dynamic imbalance—the (mis)alignment of the inertia matrix with respect to the reference coordinates. For that reason it is a purely kinematic parameter. Nutation and coning, however, involve the dynamics. Another parameter that is a measure of the inertia properties is the inertia ratio σ, sometimes known as the roll-to-pitch ratio:

$$\sigma = 1 + \text{Re}\left(\sqrt{\left(1 - \frac{I_1}{I_2}\right)\left(1 - \frac{I_1}{I_3}\right)}\right)\text{sgn}\left(I_1 - I_2\right). \tag{37}$$

This parameter indicates not only proximity to intermediate-axis spin (for which $\sigma=1$) but also determines the nutation frequency [14].

Results

The results of 2000 random simulations are shown in the following figures. First we show the results for the proposed approach to inertia statistics and then those for a more naïve approach. Figure 4 includes two histograms: one for inertia ratio and another for wobble angle. The central values, from the data in Table 1, are 1.408 and 1.144° respectively. The variation in these parameters, as we have explained, is only a function of the distribution in the principal moments of inertia. Figure 5 shows histograms of the payload and launch-vehicle inertia matrices for this approach. Figure 6 shows wobble, nutation, and coning.
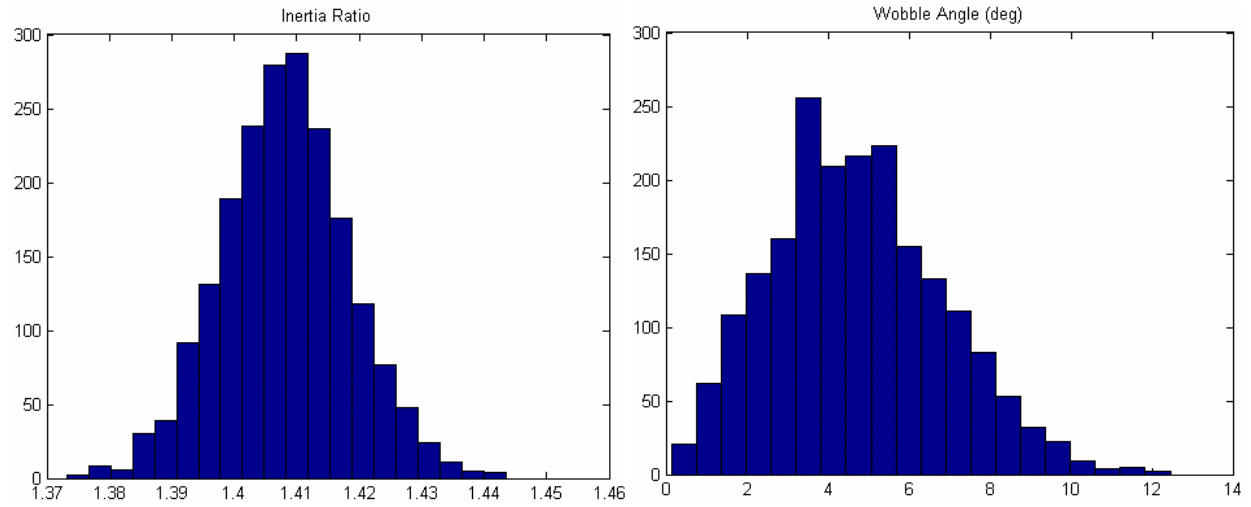
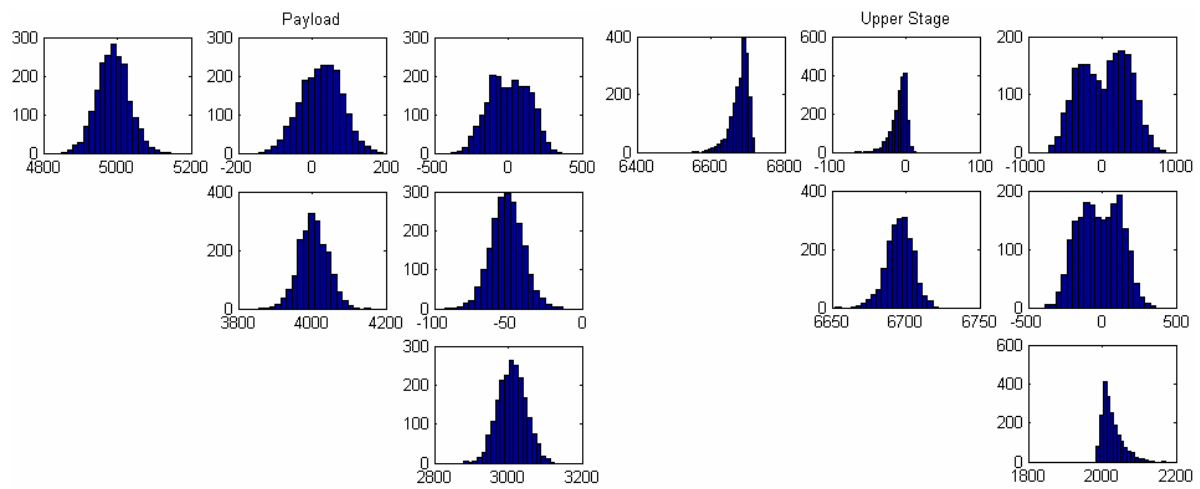Figure 4. Inertia Ratio and Wobble Angle Distributions

Figure 5. Inertia Distributions for the Payload and the Upper Stage

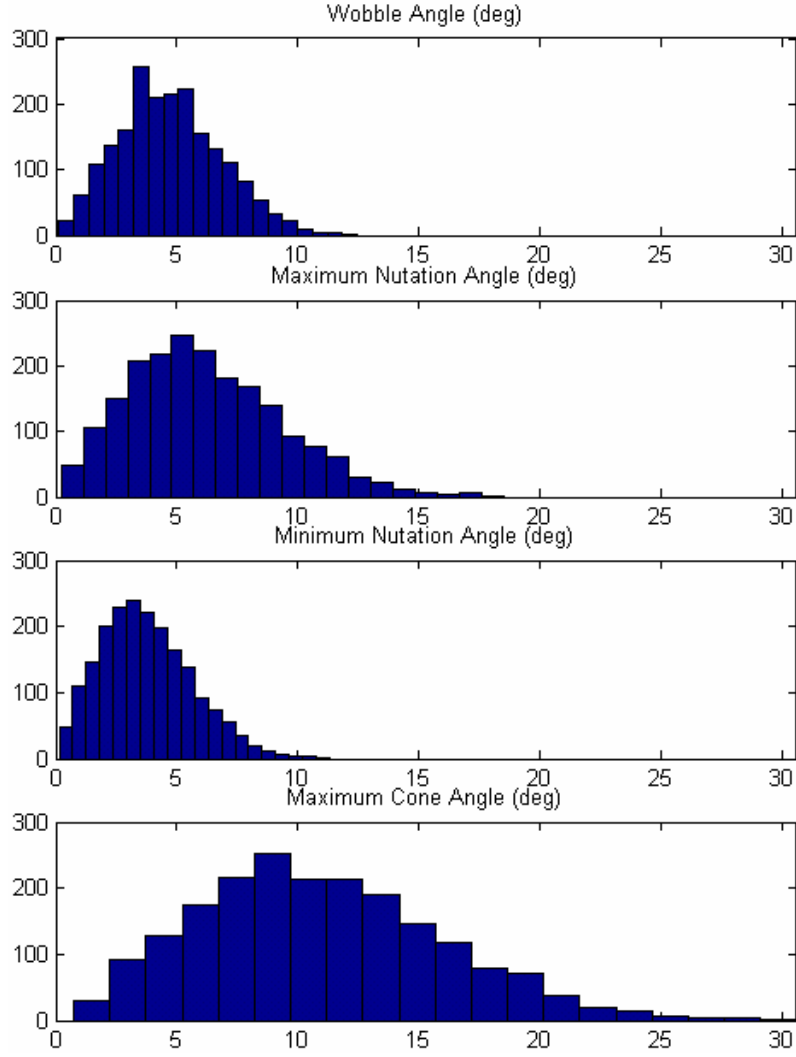(Inertia-Matrix Ordering, Symmetric Entries Omitted)

15

Figure 6. Separation Dynamics for the Proposed Uncertainty Model

A more naïve method, and a quite common one, is simply to apply Gaussian distributions to the nominal inertia parameters. For as meaningful a comparison as possible, we use the numerically computed standard deviation in the moments and products of inertia shown in Figure 5 as a description of the inertia statistics, but with no effort to weed out physically unrealizable matrices. Table 2 lists the standard deviations used in this more traditional model.

Table 2. Fit of Gaussian Statistics to Physically Realizable Inertia Matrices

(Inertia-Matrix Ordering)

Standard Deviation in I_P components	42.8518	54.3897	133.1674
	54.3897	38.6060	10.8535
	133.1674	10.8535	37.3169

Standard Deviation in I_L components	24.1620	10.3127	322.0596
	10.3127	8.8193	140.7391
	322.0596	140.7391	27.298

These standard deviations seem large, and they are if they are viewed independently. However, with the constraints among the inertia entries, these results exactly, though indirectly, describe uncertainty in the three principal moments and the three-parameter attitude description. These interrelationships are not captured when one merely randomizes the entries as if they were uncorrelated. The result of such randomization is a considerably larger variation in wobble angle and inertia ratio, as Figure 7 shows. Figure 8 shows the inertia distributions. Some components appear to vary more than they in Figure 4, but when they do it is because a Gaussian model does not fit the data well. In particular, the bimodality and one-sidedness effects evident in Figure 4 are not captured.
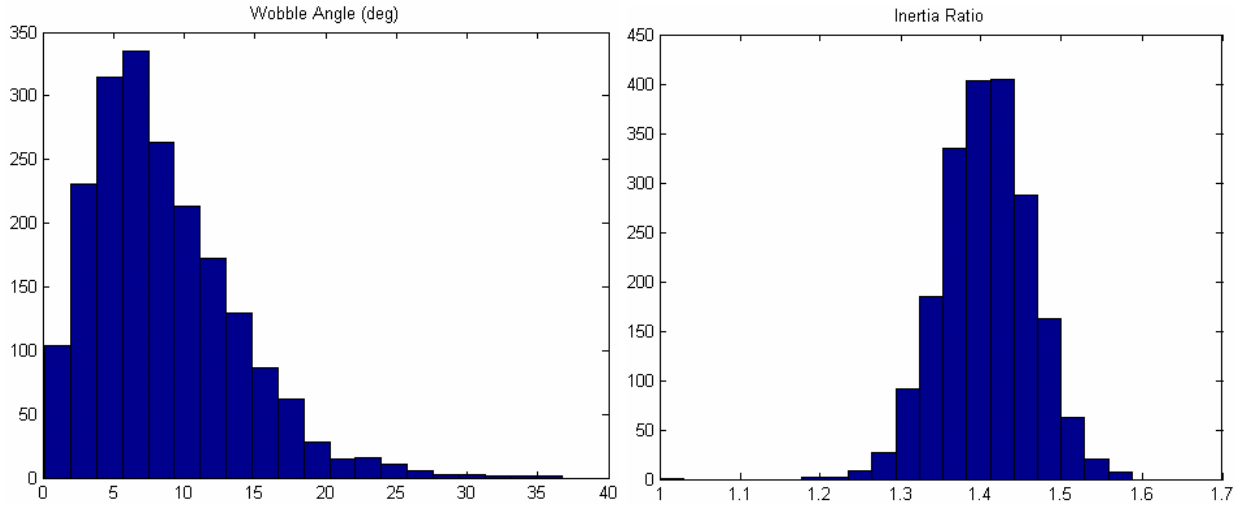

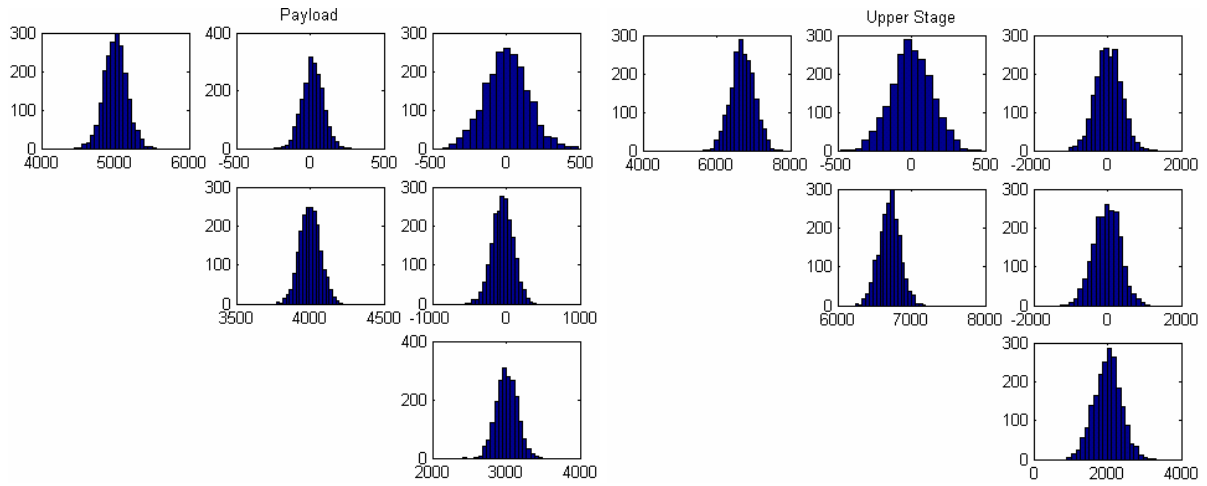Figure 7. Inertia Ratio and Wobble Angle Distributions

Figure 8. Naïve Inertia Distributions for the Payload and the Upper Stage

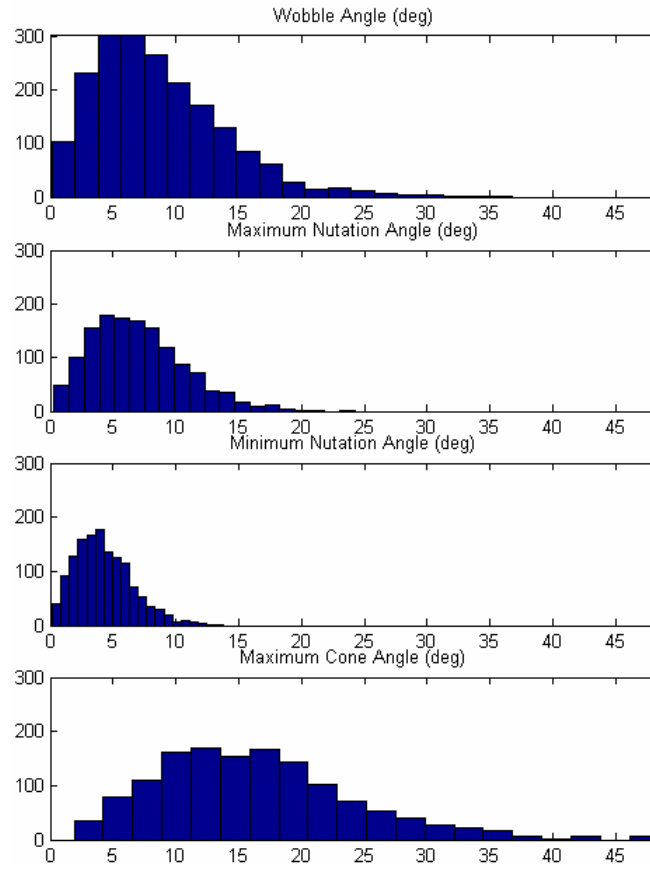(Inertia-Matrix Ordering, Symmetric Entries Omitted)

Figure 9. Separation Dynamics for the Naïve Uncertainty Model

Most important, though, is the fact that the naïve method results in considerably more variation in the separation dynamics for the same mean and standard deviation. This example makes clear that the proposed method can help extract unrealistic conservatism from some dynamics analyses.

CONCLUSIONS

We have proposed a method of representing uncertainty in inertia dyadics that is consistent with the rules governing inertia matrices. In this method, one picks random inertia matrices via normally distributed radii of gyration and normally distributed quaternions subject to a radial constraint in R^4. The distributions are not particularly intuitive, although they are fundamentally physical. They may prove useful in numerical simulation methods, such as Monte Carlo analysis. In the case of the statistical separation analysis shown as an example, this approach lead to results that reduce nutation and coning compared to a naïve approach for identical means and standard deviations in the inertia-matrix components.

REFERENCES

[1] GREENWOOD, D. T., *Principles of Dynamics*, Prentice Hall, Englewood Cliffs, New Jersey, 1988.

[2] SHUSTER, M. D., "A Survey of Attitude Representations", *Journal of the Astronautical Sciences*, Vol. 41, No. 4, pp. 439-517, October-December, 1993.

[3] ABRAMOWITZ, M. and STEGUN, I. A. (editors). *Handbook of Mathematical Functions with Formulas, Graphs, and Mathematical Tables*, 9th printing. New York: Dover, pp. 940-943, 1972.

[4] SHUSTER, M., "Man, Like these Attitudes Are Totally Random: Other Representations," AAS/AIAA Space Flight Mechanics Meeting, Santa Barbara, California, February 2001.

[5] SHUSTER, M., "Man, Like these Attitudes Are Totally Random: Quaternions," AAS/AIAA Space Flight Mechanics Meeting, Santa Barbara, California, February 2001.

[6] BAUER, R., "Uniform Sampling of SO3," Proceedings of the 2001 Flight Mechanics Symposium, NASA Goddard Space Flight Center, June, 2001.

[7] MULLER, M. E. "A Note on a Method for Generating Points Uniformly on *N*-Dimensional Spheres," *Comm. Assoc. Comput. Mach.* **2**, 19-20, 1959.

[8] AHMED, J., COPPOLA, V. T., and BERNSTEIN, D. S., "Asymptotic Tracking of Spacecraft Attitude Motion with Inertia Identification," *AIAA J. Guid. Contr. Dyn.*, Vol. 21, pp. 684-691, 1998.

[9] NICEWARNER, K. E. and SANDERSON, A. C., "A General Representation for Orientational Uncertainty Using Random Unit Quaternions," ICRA 1994: 1161-1168.

[10] CRAIG, J. J., *Introduction to Robotics*, Second Edition, Addison-Wesley, 1989.

[11] SOBOL, I. M. *A Primer for the Monte Carlo Method*. Boca Raton, FL: CRC Press, 1994.

[12] GARG, S.C, TILLEY, S. W., and PATTERSON, T. C., "Design and Development of the INTELSAT VII and VIIA Attitude Determination and Control Subsystem," AIAA Paper 93-1046, August 1993.

[13] HALL, C., "Relative Equilibria of a Gyrostat," *Journal of Guidance, Control, and Dynamics*, Vol. 20, July-Aug. 1997, pp. 625-632.

[14] HUGHES, P. C., *Spacecraft Attitude Dynamics*, John Wiley and Sons, New York, 1986.